Neurobiology of Disease 210 (2025) 106894

Contents lists available at ScienceDirect

Neurobiology of Disease

journal homepage: www.elsevier.com/locate/ynbdi

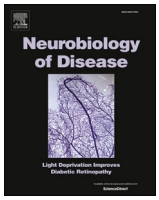

Conservation of strain properties of bank vole-adapted chronic wasting disease in the absence of glycosylation and membrane anchoring

Enric Vidal [a,b,1], Hasier Eraña [c,d,e,1], Jorge M. Charco [c,d,e], Nuria L. Lorenzo [f,l], Samanta Giler [a,b], Montserrat Ordóñez [a,b], Eva Fernández-Muñoz [c], Maitena San-Juan-Ansoleaga [c], Glenn C. Telling [g], Manuel A. Sánchez-Martín [h,i], Mariví Geijo [j], Jesús R. Requena [f,l], Joaquín Castilla [c,d,k,*]

[a] IRTA, Programa de Sanitat Animal, Centre de Recerca en Sanitat Animal (CReSA), Campus de la Universitat Autònoma de Barcelona (UAB), Bellaterra, Catalonia. Spain
[b] Unitat mixta d'Investigació IRTA-UAB en Sanitat Animal, Centre de Recerca en Sanitat Animal (CReSA), Campus de la Universitat Autònoma de Barcelona (UAB), Bellaterra, Catalonia. Spain
[c] Center for Cooperative Research in Biosciences (CIC BioGUNE), Basque Research and Technology Alliance (BRTA), Derio, Spain
[d] Centro de Investigación Biomédica en Red de Enfermedades infecciosas (CIBERINFEC), Carlos III National Health Institute, Madrid, Spain
[e] ATLAS Molecular Pharma S. L., Derio, Spain
[f] CIMUS Biomedical Research Institute, University of Santiago de Compostela-IDIS, Santiago de Compostela, Spain
[g] Prion Research Center, Colorado State University, Fort Collins, USA
[h] Transgenic Facility, Department of Medicine, University of Salamanca, Salamanca, Spain
[i] Institute of Biomedical Research of Salamanca (IBSAL), Salamanca, Spain
[j] Animal Health Department, NEIKER-Basque Institute for Agricultural Research and Development, Basque Research and Technology Alliance (BRTA), Derio, Spain
[k] IKERBASQUE, Basque Foundation for Science, Bilbao, Spain
[l] Department of Medical Sciences, University of Santiago de Compostela-IDIS, Santiago de Compostela, Spain

ARTICLE INFO

Keywords:
Prion
Transmissible spongiform encephalopathies
Chronic wasting disease
Glycosylation
Prion strains

ABSTRACT

Prion disease phenotypes (prion strains) are primarily determined by the specific misfolded conformation of the cellular prion protein (PrP^C). However, post-translational modifications, including glycosyl phosphatidyl inositol (GPI) membrane anchoring and glycosylation, may influence strain characteristics. We investigated whether these modifications are essential for maintaining the unique properties of bank vole-adapted Chronic Wasting Disease (CWD-vole), the fastest known prion strain. Using a novel transgenic mouse model expressing I109 bank vole PrP^C lacking the GPI anchor and largely devoid of glycans, we performed serial passages of CWD-vole prions. Despite elongated initial incubation periods, the strain maintained 100 % attack rate through three passages. Although the pathological phenotype showed characteristic GPI-less features, including abundant extracellular plaque formation, three subsequent serial passages in fully glycosylated and GPI-anchored bank vole I109 PrP^C expressing transgenic mice TgVole (1×) demonstrated that the strain's distinctive rapid propagation properties were preserved. These findings suggest that neither GPI anchoring nor glycosylation are essential for maintaining CWD-vole strain properties, supporting the concept that strain characteristics are primarily encoded in the protein's misfolded structure.

* Corresponding author.
E-mail addresses: enric.vidal@irta.cat (E. Vidal), herana.atlas@cicbiogune.es (H. Eraña), jmoreno@cicbiogune.es (J.M. Charco), nuria.lopez.lorenzo2@usc.es (N.L. Lorenzo), samanta.giler@irta.cat (S. Giler), montserrat.ordonez@irta.cat (M. Ordóñez), efernandez@cicbiogune.es (E. Fernández-Muñoz), msanjuan.visitor@cicbiogune.es (M. San-Juan-Ansoleaga), glenn.Telling@colostate.edu (G.C. Telling), adolsan@usal.es (M.A. Sánchez-Martín), mgeijo@neiker.eus (M. Geijo), jesus.requena@usc.es (J.R. Requena), castilla@joaquincastilla.com (J. Castilla).
[1] These authors contributed equally to this work.

https://doi.org/10.1016/j.nbd.2025.106894
Received 29 January 2025; Received in revised form 28 March 2025; Accepted 28 March 2025
Available online 11 April 2025

1. Introduction

Prion diseases are a group of fatal neurodegenerative disorders affecting humans and animals. The most relevant include Creutzfeldt-Jakob disease (CJD) in humans, bovine spongiform encephalopathy (BSE) in cattle, scrapie in small ruminants, and chronic wasting diseases (CWD) in cervids (Parchi and Gambetti, 1995; Wells et al., 1987; Williams, 2005). Prion diseases are classified as protein misfolding diseases since their common pathogenic mechanism is the conformational change of the host-encoded cellular prion protein (PrP^{C}) into a pathological misfolded state (Prusiner, 1991).

Prion diseases are characterized by a noticeable phenotypic variability, not only among different species abut also within a single species. This phenomenon in which minor structural differences in the misfolding of a single protein yields a distinct disease phenotype is described as "prion strains" (Collinge and Clarke, 2007). The mechanisms driving prion strain's biological outcomes are yet unknown. The biological determinants of the differential brain lesion and prion protein deposit distribution, the relative proportions of glycoforms, the incubation periods in animal models or the capacity to cross certain species barriers remain still unexplained. All these properties seem to be encoded in the distinct tertiary and/or quaternary structural organization of each prion conformer (Hoyt et al., 2022; Kraus et al., 2021; Manka et al., 2023a, 2023b).

One of the defining features of prion strains is the velocity with which prions propagate within the central nervous system of an infected subject, some of them showing a fast distribution pace while others are slower. Among the rapid progressing prions, we can highlight the bank vole (BV)-adapted CWD strain (CWD-vole) obtained after the experimental intracerebral inoculation of an elk (*Cervus canadiensis*) CWD isolate in bank voles (*Myodes glareolus*) presenting the I109 polymorphism in the PrP. This strain has the ability to cause terminal disease in its host in around 35 days after intracerebral inoculation being the fastest prion strain ever described (Di Bari et al., 2013). Bioassays in transgenic mouse models expressing BV PrP^{C} confirm the fast-spreading capabilities of CWD-vole prions and that these are not exclusively explained by the genetic background of *Myodes glareolus*, since it can happen also in a mouse background (Otero et al., 2019).

Another feature of prion strains that has been widely explored in the field is the glycosylation of the prion protein. The cellular prion protein undergoes several post-translational modifications in the endoplasmic reticulum (ER), including the attachment of two N-linked glycans and a glycosyl phosphatidyl inositol (GPI) moiety at the C-terminus. PrP^{C} is then further processed in the Golgi apparatus where the N-linked oligosaccharides are modified to include complex sugar moieties. It is subsequently moved to the cell surface, where it is attached to detergent-resistant lipid rafts on the outer membrane of the cell through the GPI anchor. The number of glycans attached to PrP^{C} can vary, resulting in the di-, mono-, or unglycosylated forms of the protein, and the proportion of each of these glycoforms can vary with each prion strain (Lawson et al., 2005; Rudd et al., 2002).

The implication of the GPI anchoring of PrP^{C} to the membrane on the pathogenesis of prion diseases has been extensively studied using transgenic mouse models expressing PrP^{C} without the GPI anchor (Chesebro et al., 2005; Watts et al., 2016). Bioassays in these mice showed that anchorless PrP could still be misfolded, templated by the inoculated prion strain; however, its pathogenesis was altered, and the incubation period significantly delayed. The altered location of misfolded, proteinase-resistant PrP (PrP^{res}) in this model, shed in the brain interstitial fluid instead of being anchored to the membrane, prevented the usual neuronal spread of prions within the brain and shifted it to the brain interstitial fluid draining pathways, thus accumulating extracellularly in the perivascular, subependymal, and submeningeal spaces (Rangel et al., 2014). Interestingly, the loss of the GPI in prions propagated in that transgenic model was later demonstrated to have altered the features of some experimental strains (mouse-adapted CWD), whereas others remained unchanged (ME7, RML, or 22L) in terms of both incubation period and morphology of PrP^{res} deposits when back-passaged in wild-type mice (Aguilar-Calvo et al., 2017).

In vitro studies showed that unglycosylated, GPI-less recombinant human PrP (recPrP) is capable of blocking PrP^{C} conversion into PrP^{res} in PMCA reactions (Yuan et al., 2013), and this result was replicated with hamster recPrP (Kim et al., 2009). Also, removal of the GPI anchor with phosphatidylinositol-specific phospholipase C (PI-PLC) yielded normal brain homogenates unable to propagate misfolded, disease-associated PrP (PrP^{Sc}) seeds *in vitro*, highlighting the relevance of the GPI in the conversion process, probably related to its role in the location of PrP^{C} in the cellular membrane (Kim et al., 2009). On the other hand, a stop codon mutation in the gene encoding for PrP has been described to elicit a Gerstmann-Sträussler-Scheinker syndrome (GSS) phenotype in patients with anchorless PrP^{res} (Jansen et al., 2010; Shen et al., 2021), associated with prion protein amyloid angiopathy. Despite numerous evidence showing that misfolded recombinant prion proteins ($recPrP^{Sc}$) can propagate in various environments, both *in vivo* and *in vitro* (Eraña et al., 2024) there is no evidence to suggest that the absence of glycans and GPI allows for the maintenance of specific strains when they are propagated in a recombinant environment.

The study of PrP^{C} glycosylation has attested to its relevance in many aspects of prion diseases pathogenesis, including, but not limited to, lymphotropism, brain area tropism of different strains, and neuroinflammatory responses (Makarava and Baskakov, 2023). Transgenic mouse expressing non-glycosylated PrP^{C} can be infected, and the resulting strain is then infectious to wild-type mice, proving that glycosylation is not essential for prion replication, even though its absence profoundly alters transmission properties (Tuzi et al., 2008). Relevant differences were also noted between strains. For instance, while 79A was infectious to mice expressing non-glycosylated PrP^{C}, ME7 was not. However, ME7 was infectious to mice expressing PrP^{C} with one glycan at position N196 but not to those which lacked glycosylation at the N180 position (Tuzi et al., 2008). Host glycosylation has also been proven to be a strong determinant of the interspecies transmission barrier (Wiseman et al., 2015) and to influence neuroinvasion after peripheral inoculation of ME7 and 79A scrapie strains and their neuroanatomical PrP^{res} distribution in the brain (Cancellotti et al., 2010). However, de-glycosylated PrP^{Sc} has been shown to maintain the strain specific neurotropism of both RML and 301C prions (Piro et al., 2009). Similarly, several BSE derived prion isolates have been shown to maintain their pathobiological features after either *in vitro* or *in vivo* passage through a non-glycosylated human PrP^{C}-expressing mouse model (TgNN6h) (Otero et al., 2022).

Understanding whether the GPI anchor and the glycosylation of PrP^{C} are essential for maintaining the extraordinary propagation speed of the fastest known prion strain has a fundamental relevance in the prion field, providing insights into the molecular determinants responsible for the unique propagative properties of bank vole-adapted CWD, while also having important practical implications for structural studies, particularly given that recent breakthroughs in cryo-EM characterization of prion strains have relied on proteins lacking these post-translational modifications. Therefore, we conducted serial passages in our novel bank vole GPI-less transgenic mouse model followed by back-passages into the TgVole (1×) mice (Eraña et al., 2019) to comprehensively assess the role of post-translational modifications in strain stability.

2. Materials and methods

2.1. Generation of a transgenic mouse model expressing bank vole GPI-less PrP^{C}

After isolation by PCR amplification from genomic DNA, extracted using GeneJET™ Genomic DNA Purification Kit (Fermentas) from a bank vole brain tissue sample using 5′ CCGGAATTCCGGCGTACGATGGCGAACCTCAGCTAC 3′ and 5′

GTCTAGACTAGGCCGGCCTTAGGAACTTCTCCCTTCGTAG 3′ as primers, the open reading frame (ORF) of the bank vole *PRNP* gene with I109 polymorphism with a STOP codon after residue 231 was cloned into the pDrive vector (Qiagen).The ORF from, the GPI-less bank vole I109-PrP was excised from the cloning vector by using the restriction enzymes *Bsi*WI (Thermo Fisher Scientific Inc.) and *Fse*I (New England Biolabs Ltd.) and then inserted into a modified version of MoPrP.Xho vector (Borchelt et al., 1996) as described previously (Castilla et al., 2005), which was also digested with BstWI and FseI. This vector contains the murine PrP promoter and exon-1, intron-1, exon-2 and 3′ untranslated sequences. Finally, the construct was excised using *Not*I enzyme and purified with an Invisorb Spin DNA Extraction Kit (Inviteck) according to the manufacturer recommendations.

Transgenic mouse founders of the C57Bl6 x CBA background were generated by microinjection of NotI excised DNA into pronuclei following standard procedures (Castilla et al., 2003). DNA extracted from tail biopsies was analyzed by PCR using specific primers for the mouse exon 2 and 3′ untranslated sequences (5′ GAACTGAACCATTTCAACCGAG 3′ and 5′ AGAGCTACAGGTGGATAACC 3′). Those which tested positive were bred to mice null for the mouse *Prnp* gene in order to avoid endogenous expression of mouse prion protein. Absence of the mouse endogenous *Prnp* was assessed using the following primers: 5′ ATGGCGAACCTTGGCTACTGGC 3′ and 5′ GATTATGGGTACCCC CTCCTTGG 3′. Bank vole PrP^{C} expression levels of brain homogenates from transgenic mouse founders were determined by Western blot using anti-PrP Sha31 (1:4000) monoclonal antibody (Cayman Chemical) and compared with the PrP expression levels from a C57/BL6 WT mouse brain homogenate (Supplemental Figs. S1 and S2).

The international code to identify this transgenic mouse lines is B6&CBA.129Ola-Tg(Prnp-Vo109I-GPILess)1Sala/Cicb although throughout the article it is referred to as TgVole-GPI-less.

2.2. Mouse bioassays

Inocula were prepared as a 10 % (w/v) homogenate in PBS of either TgVole (1×) mice inoculated with CWD-vole provided by Romolo Nonno, ISZ, Rome (Di Bari et al., 2013) or 10 % (w/v) in PBS from a single, TSE-confirmed, mouse brain form each bioassay, selecting the brain homogenate of an animal from each group showing an incubation period as close as possible to the mean of the group and good PrP^{res} signal assessed by Western blotting.

Mice of 42–56 days of age were intracerebrally inoculated, under intraperitoneal anesthesia [ketamine/medetomidine (75/1 mg/kg, Imalgene 1000, Boehringer Ingelheim/ Domtor, Ecuphar)] reversed with atipamezole hydrochloride (1 mg/kg, Antisedan, Ecuphar), through the right parietal bone, with a 27G needle (Terumo) to inoculate a volume of 20 μl. Mice were kept in a controlled environment at a room temperature of 22 °C, 12 h light-darkness cycle and 60 % relative humidity in HEPA filtered cages (both air inflow and extraction) in ventilated racks. The mice were fed *ad libitum*, observed daily and their clinical status assessed twice a week. The presence of TS*E*-associated clinical signs was scored. Positive TSE diagnosis relied on the detection of PrP^{res} (by either immunohistochemistry and/or Western blotting) and associated spongiform changes on stained histological sections of the brain parenchyma.

2.3. PrP^{Sc} detection by electrophoresis and Western blot

Proteinase K digestion of brain homogenate samples: For PrP^{Sc} detection in brain homogenates from inoculated animals, proteinase K (PK) digestion was performed prior to Western blotting. For that, brains of inoculated animals homogenized at 10 % (w/v) in Phosphate buffered saline (PBS) (Fisher Bioreagents) with Protease inhibitor cocktail (Roche), were mixed with digestion buffer [2 % (w/v) Tween-20 (Sigma-Aldrich), 2 % (v/v) NP-40 (Sigma-Aldrich) and 5 % (w/v) Sarkosyl (Sigma-Aldrich) in PBS] at 1:1 (v/v). PK (Roche) was added to each sample to reach a final concentration of 170 μg/ml, and these were incubated at 42 °C for 1 h at 450 rpm of shaking in a thermomixer (Eppendorf). Digestion was stopped by adding loading buffer (NuPage 4× Loading Buffer, Invitrogen) 1:3 (v/v) and boiling samples for 10 min at 100 °C. For the detection of PrP^{Sc} with atypical biochemical signature, we based on a procedure described previously (Wenborn et al., 2015). Briefly, 10 % brain homogenates were digested with Pronase E (Sigma-Aldrich) at 100 μg/ml for 30 min at 37 °C and vigorous shaking (800 rpm). After addition of EDTA (Calbiochem) for a final concentration of 10 mM and Sarkosyl for a final 2 % (w/v) concentration, Pronase E-digested samples were further processed with Benzonase (Merck) at 50 U/ml for 10 min at 37 °C and 800 rpm. Then, sodium phosphotungstic salt (NaPTA) (Sigma-Aldrich) was added at 0.3 % (w/v) and samples incubated for 30 min at 37 °C and 800 rpm. Upon addition of iodixanol 60 % (OptiPrep density gradient medium, Sigma-Aldrich) and NaPTA, for final concentrations of 35 % (w/v) and 0.3 % (w/v), respectively, samples were centrifuged at 16,100*g* for 90 min and supernatant (avoiding flocculants) transferred to a new tube after filtration through 0.45 μm pore-size microcentrifuge filtration units (Millipore). These supernatants were afterwards mixed 1:1 with a buffer composed by 2 % Sarkosyl (w/v) and 0.3 % NaPTA diluted in PBS. After an additional 90 min centrifugation at 16,100*g* the supernatant was discarded, and pellet resuspended in washing buffer [iodixanol 17.5 % (w/v) and Sarkosyl 0.1 % (w/v) in PBS]. The resuspended pellets were then digested with Proteinase K at a final concentration of 10 μg/ml for 1 h at 37 °C and 800 rpm. After adding washing buffer and NaPTA for a final concentration of 0.3 % (w/v), samples were once more centrifuged at for 30 min at 16,100*g* and supernatants discarded. This step was repeated, and the final pellet resuspended in loading buffer (NuPage 4× Loading Buffer, Invitrogen) 1:3 (v/v).

Western blot: Digested samples, together with non-digested controls, were boiled at 100 °C for 10 min prior to loading in 4–12 % acrylamide gels (*NuPAGE Midi gel*, Invitrogen Life Technologies) for 1 h 20 min (10 min at 70 V, 10 min at 110 V and 1 h at 150 V). Samples were then transferred to PVDF membranes through the iBlot™ 3 (Invitrogen), that were then developed using the iBind™ Flex Western Device (Invitrogen) and Sha31 (1:4000) monoclonal antibody (Cayman Chemical). After incubation with peroxidase-conjugated secondary anti-mouse antibody (m-IgGκ BP-HRP, Santa Cruz Biotechnology), membranes were developed with an enhanced chemiluminescent horseradish peroxidase substrate (West Pico Plus, Thermo Scientific), using an iBright™ CL750 imaging system (Invitrogen) for image acquisition and the software AlphaView (Alpha Innotech) for image processing. In some cases, anti-α-tubulin mAb (1:16,000) (Sigma-Aldrich) was also used as primary antibody to develop the membranes to control the amount of brain homogenate loaded in each case.

2.4. Anatomopathological analysis and immunohistochemistry

Transversal sections of each half brain fixed in formalin were performed at the levels of the medulla oblongata, piriform cortex and optic chiasm. All sections were then embedded in paraffin-wax after dehydration through increasing alcohol concentrations and xylene. Sections of four micrometres were placed on glass microscope slides and stained with haematoxylin (Sigma) and eosin (Casa Álvarez) (H&E). Additional sections were mounted in 3-trietoxysilil-propilamine-coated glass microscope slides (Dako) for immunohistochemistry, as described previously (Vidal et al., 2022). Treated tissue sections were deparaffinized and subjected to epitope unmasking treatments: immersion in formic acid and boiling (at pH 6.15) in a pressure cooker and pre-treating them with 4 μg/ml of proteinase K (Roche). Endogenous peroxidases were blocked by immersion in a 3 % H_2O_2 in methanol solution. Sections were then incubated overnight with anti-PrP monoclonal antibody 6C2 (1:1000, CVI-Wageningen UR) or exceptionally with 2G11 (1:100, Bertin Pharma), and visualized using the Goat anti-mouse EnVision system (DAKO) and 3,3′-diaminobenzidine (Sigma Aldrich). As a

background control, incubation with the primary antibody was omitted. Brain histological lesions, spongiform change and PrP^{res} immunolabeling, were evaluated under a light microscope. Using a semi-quantitative approach (Vidal et al., 2022), spongiform lesion and PrP^{res} immunolabeling were separately scored in fourteen different brain regions: piriform cortex (Pfc), hippocampus (H), occipital cortex (Oc), temporal cortex (Tc), parietal cortex (Pc), frontal cortex (Fc), striatum (S), thalamus (T), hypothalamus (HT), mesencephalon (M), medulla oblongata (Mobl), cerebellar nuclei (Cm), cerebellar vermis (Cv) and cerebellar cortex (Cc). Scores ranging from (0) absence of spongiosis or immunolabeling: (1) mild, (2) moderate, (3) intense and (4) maximum intensity of lesion or immunolabeling were assigned to each brain area studied, that was investigated globally as region for the scoring. Brain profiles were plotted as a function of the anatomical areas which were ordered representing the caudo-rostral axis of the encephalon. Graphs were plotted using Microsoft Office Excel software.

3. Results

3.1. Generation of a transgenic mouse model expressing bank vole GPI-less PrP^C

To investigate the role of post-translational modifications in CWD-vole strain properties, we generated a transgenic mouse model expressing bank vole PrP^C lacking the GPI anchor attachment signal. The transgenic construct was designed based on our previous models, with key modifications to prevent GPI anchoring. The construct contained the mouse PrP promoter and the bank vole *PRNP* open reading frame (ORF) with the I109 polymorphism, modified by introducing a stop codon immediately after residue 231 to prevent GPI anchor attachment signal translation. The absence of this signal alters the biosynthetic pathway of the PrP^C, resulting in mostly unglycosylated protein. Four founder lines were obtained and successfully transmitted the transgene to their progeny. These lines were backcrossed with *Prnp*$^{-/-}$ mice (Manson et al., 1994) to eliminate endogenous PrP expression. Western blot analysis of brain homogenates from the different lines revealed varying PrP^C expression levels. We selected one line, designated TgVole-GPI-less, showing homozygous PrP^C expression at 0.25× compared to wild-type bank voles. This relatively low expression level is consistent with other GPI-less transgenic models previously published (Chesebro et al., 2005; Stöhr et al., 2011). As expected, biochemical characterization demonstrated both the absence of glycosylation and a lower molecular weight of the protein due to the lack of the GPI anchor (Supplemental Fig. S1). The altered post-translational modifications band pattern confirms the successful disruption of the normal biosynthetic pathway in this model.

The presence of isoleucine at position 109 of bank vole PrP has been consistently associated with spontaneous prion disease development in transgenic models with onset timing correlating inversely with PrP^C expression levels (Otero et al., 2021; Vidal et al., 2022; Watts et al., 2016). However, TgVole-GPI-less mice showed remarkable stability, with lifespans comparable to wild-type animals and no detectable clinical phenotype. Only sporadic cases presented extensive extracellular PrP^{res} deposits at advanced ages (> 700 days), likely reflecting the protective effect of the model's low PrP^C expression levels combined with the absence of membrane anchoring, which may reduce the efficiency of spontaneous misfolding events.

In summary a new mouse model was generated expressing GPI-less and mostly unglycosylated bank vole PrP^C in a murine knockout background.

3.2. The fastest known prion strain propagates in TgVole-GPI-less

To assess whether this strain could maintain its distinctive properties in the absence of post-translational modifications, we challenged TgVole-GPI-less with the previously described bank vole-adapted CWD strain (CWD-vole) (Di Bari et al., 2013).The first passage showed complete penetrance, with all animals developing disease signs by 618 ± 7 dpi (mean ± SEM) (Table 1). Clinical manifestations suggestive of neurological impairment were first observed in one animal at 591 dpi, although these signs were partially masked by age-related conditions in this and all other animals in the group. Despite the extended incubation period, which was expected given the low PrP^C expression levels, the prolonged clinical phase allowed for substantial accumulation of PK-resistant PrP (PrP^{res}) with a distinctive migration pattern reflecting the lack of glycosylation (Fig. 1 and Supplemental Fig. S3). Histopathological examination showed mild spongiosis mixed with age-related spongiosis. Visible amyloid plaques were observed not associated with this spongiform change. Immunohistochemical analysis revealed widespread small extracellular PrP^{res} plaques with radial organization (Fig. 2). These plaques predominantly accumulated in perivascular, submeningeal, and subependymal spaces, showing a broad distribution throughout the brain with higher density in the neocortex, paleocortex, and hippocampus. The isolate obtained from the brains of these mice was named CWD-vole GPI-less-1p.

A second passage was conducted to evaluate strain adaptation to the GPI-less environment. Animals were euthanized at 455 dpi following general body condition decline, despite the absence of clear neurological signs. Biochemical and histopathological analysis revealed again a 100 % attack rate. The spongiform pattern remained consistent with the first passage, showing mild changes accompanied by prominent senile spongiosis. However, immunohistochemistry revealed a marked increase in PrP^{res} accumulation, with plaque-like deposits visible even in H&E staining and a threefold increase in PrP^{res} immunostaining scores compared to the first passage (Fig. 2). The characteristic biochemical pattern of PK-resistant PrP remained unchanged (Fig. 1). The resulting isolate was subsequently named CWD-vole GPI-less-2p.

A third passage was conducted to confirm strain adaptation to the

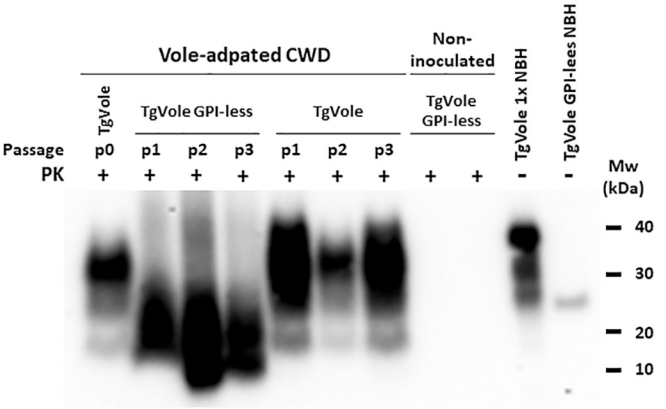

Fig. 1. Biochemical analysis of the PrP^{Sc} from the TgVole GPI-less and the TgVole animals sequentially inoculated with the bank vole-adapted CWD prion strain. A representative example from animals of each passage performed to adapt the vole-CWD prion strain to TgVole GPI-less model (p1, p2 and p3) and back-passages to TgVole (p1, p2 and p3), expressing GPI-anchored and fully glycosylated PrP^C are shown as analyzed by proteinase K digestion and Western blot using monoclonal antibody Sha31 (1:4000). The original inoculum, obtained from a CWD-vole infected TgVole (p0 TgVole) is also included in the gel together with the analysis of the brains of two non-inoculated TgVole GPI-less mice, negative for PrP^{Sc}. Undigested controls of brain homogenates from both models are also shown as size references. CWD-vole inoculated TgVole GPI-less mice, as expected show a PrPSc fragment corresponding to the non-glycosylated form of PrP, slightly lower than the unglycosylated fragment from TgVole animals due to the absence of the GPI-anchor. The product resulting of the adaptation of this GPI-less prions back to TgVole are indistinguishable from the original inoculum, with identical protease resistant core size and predominant diglycosylated fragment. PK: Proteinase K; Mw: Molecular weight. Uncropped blot provided as a .tiff file named Supplemental Fig. S3.

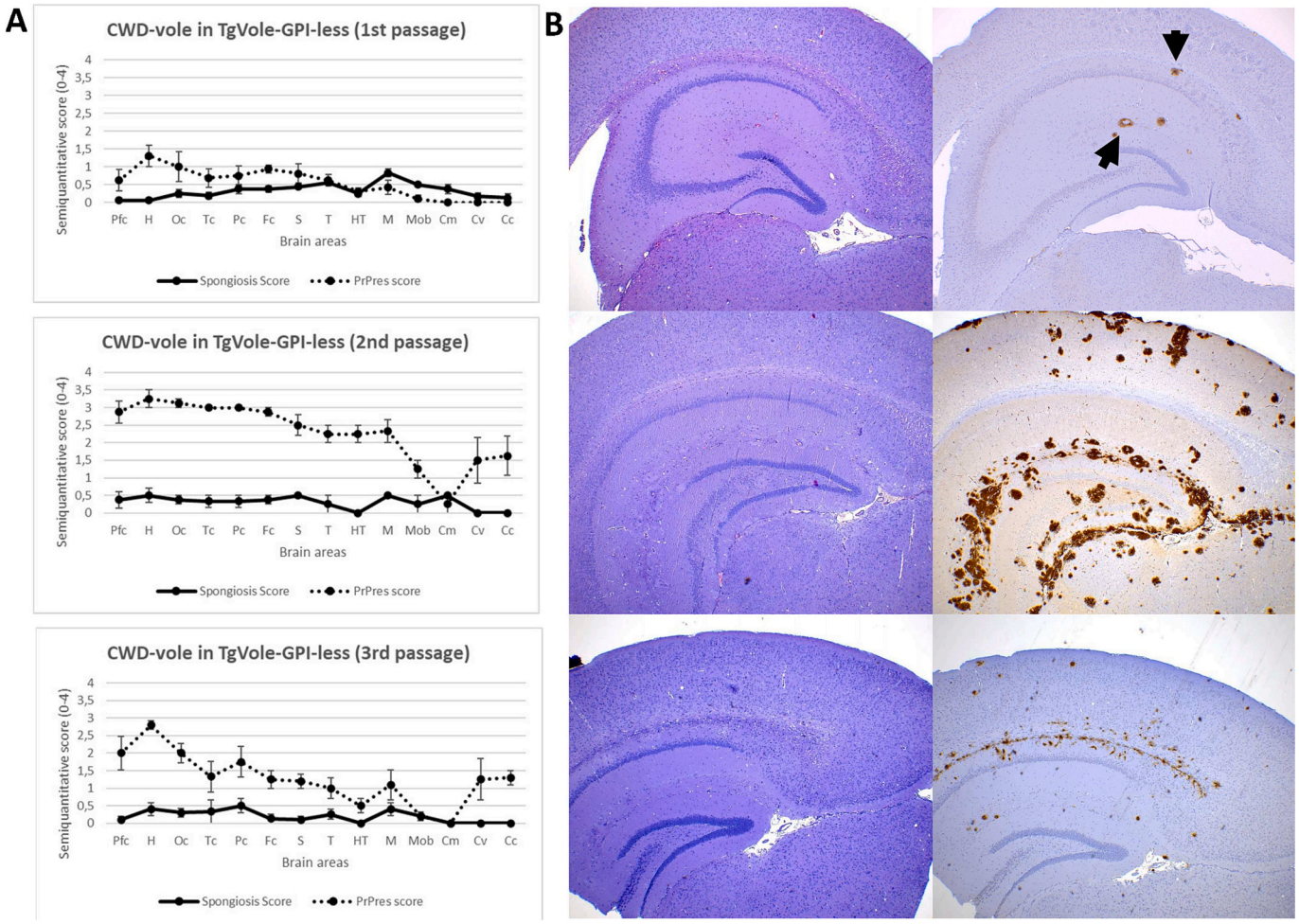

Fig. 2. Neuropathological characterization of serial bioassays of bank vole adapted CWD in the TgVole-GPI-less mouse model. **A)** Brain lesion and PrP^{res} deposit distribution profiles for the three sequential bioassays of CWD-vole in TgVole-GPI-less mice. Brain lesion profiles and PrP^{res} deposition profiles represent the mean semi-quantitative scoring (0 -absence of lesion- to 4 -maximum intensity-, vertical axis) and error bars are the standard error of the mean of the spongiform lesions (continuous black line) and the immunohistochemical labelling of PrP^{res} deposits (dashed line) against 14 brain regions (Pfc: piriform cortex, H: hippocampus, Oc: occipital cortex, Tc: temporal cortex, Pc: parietal cortex, Fc: frontal cortex, S: striatum, T: thalamus, HT: hypothalamus, M: mesencephalon, Mob: medulla oblongata, Cm: cerebellar nuclei, Cv: cerebellar vermis, Cc: cerebellar cortex). **B)** Haematoxylin-eosin staining of the hippocampus of representative mice evidencing mild to absent spongiform lesion on the left column and, on the right column, PrP^{res} immunostaining with the monoclonal antibody 6C2 (1:1000) where extracellular plaques are stained in brown (arrows). A few plaques were observed on the first passage, while a higher number and bigger in size on the second passage and, on the third passage, a similar number but smaller in size, likely because the animals were culled before terminal disease. Each image corresponds to a representative animal of the graph in panel A, on the left. (For interpretation of the references to colour in this figure legend, the reader is referred to the web version of this article.)

Table 1
Sequential intracerebral inoculation of CWD-vole prion strain in TgVole-GPI-less mice and TgVole (1×) mice.

Strain	Model	1st passage			2nd passage			3rd passage		
		Attack rate	Days post-inoculation (± SEM)	PrP^{Sc} classic pattern (WB/IHC)	Attack rate	Days post-inoculation (± SEM)	PrP^{Sc} classic pattern (WB/IHC)	Attack rate	Days post-inoculation (± SEM)	PrP^{Sc} classic pattern (WB/IHC)
CWD-vole	TgVole GPI less	8/8	618 ± 7	8/8	4/4	455 ± 0	4/4	5/5	326 ± 32[a]	5/5
CWD-vole-GPI-less-3p	TgVole (1×)	5/5	82 ± 3	5/5	6/6	64 ± 3	6/6	5/5	67 ± 3	5/5
CWD-vole	TgVole (1×)	6/6	58 ± 2	6/6						

SEM: Standard error of the mean. WB: Western blotting, IHC: immunohistochemistry.
[a] Euthanized before onset of clinical signs.

TgVole-GPI-less model. Animals were culled at 326 ± 32 dpi, with initial euthanasia of two animals due to concurrent neoplastic disease. These animals tested positive for TSE by both WB and immunohistochemistry (IHC), prompting euthanasia of the remaining group upon early signs of body condition decline, despite the absence of clear neurological signs. All animals showed PK-resistant PrP^{res}, maintaining a 100 % attack rate even in those euthanized earlier due to neoplasia. Histopathological examination revealed minimal to absent spongiform change, while

PrP^{res} deposits maintained a distribution pattern similar to the second passage but with notably smaller plaques, likely due to the ~129 days shorter survival period (Fig. 2). The combination of shortened incubation time and consistent PrP^{res} distribution pattern, despite reduced plaque size, suggested successful strain adaptation to the GPI-less environment. The resulting isolate of this passage was named CWD-vole-GPI-less-3p.

In summary, the CWD-vole strain successfully infected the new TgVole-GPI-less model, albeit with long incubation periods, through three serial passages, fully adapting to the GPI-les environment and showing a distinct phenotype, similar to that observed in other GPI-less models.

3.3. Anchorless and non-glycosylated CWD-vole strain retained its pathobiological features upon back passage to TgVole (1×) mice

After adaptation to the GPI-less environment, we investigated whether the strain maintained its original properties by performing back passages into TgVole (1×) mice expressing fully glycosylated, GPI-anchored bank vole I109 PrP. The initial back passage showed complete penetrance, with all animals succumbing to disease at 82 ± 3 dpi. To ensure complete strain stabilization and rule out potential transmission barriers between models, we performed two additional passages. Both showed 100 % attack rates with shortened incubation periods of 64 ± 3 dpi and 67 ± 3 dpi. There was no statistically significant difference between this, and the incubation period observed for the original CWD-vole strain (58 ± 2 dpi) (Table 1) (Kruskal-Wallis test, p-value = 0.061).

Clinical and biochemical characterization of the back passages revealed consistent disease features across all three bioassays. All animals developed typical prion disease clinical signs including kyphosis, rough coat, and gait abnormalities. Biochemical analysis showed proteinase K-resistant PrP with a classical three-band migration pattern identical to that observed in control CWD-vole infected TgVole (1×) mice (Fig. 1).

The neuropathological analysis revealed a temporal evolution of lesion patterns. In the first back passage, animals showed moderate thalamic spongiosis and minimal changes in mesencephalon and medulla oblongata, consistent with classical CWD-vole infection in TgVole (1×) mice (Fig. 3A and B). However, three out of five animals also displayed distinctive features: moderate hippocampal spongiosis and small PrP^{res}-positive plaques in the alveus layer (Fig. 3C). Additionally, the thalamus showed a subtle intracellular punctate pattern, visible only at high magnification (40×) (Fig. 3B, inserts).

These distinctive hippocampal features disappeared in subsequent passages, with second and third passage animals showing only the characteristic CWD-vole pattern: mild spongiosis in thalamus and mesencephalon, accompanied by fine intraneuronal punctate PrP^{res} deposits in thalamus, mesencephalon, and medulla oblongata. This final profile was indistinguishable from that of classical CWD-vole infection in TgVole (1×) mice (Fig. 3A and B). A comprehensive overview of the experimental design is provided in Supplemental Fig. S4.

In summary, serial back passages of the GPI-less adapted CWD-vole strain into TgVole(1×) mice showed that the lesion profile remained unaltered.

4. Discussion

We have generated a novel transgenic mouse model expressing GPI-less bank vole PrP^{C} that recapitulates key features of previously described anchorless PrP^{C} models, including low PrP^{C} expression levels and minimal glycosylation (Bett et al., 2013; Chesebro et al., 2005; Rangel et al., 2014; Stöhr et al., 2011). This characteristics stem from the absence of the GPI anchor, which normally directs PrP^{C} through the Golgi apparatus where post-translational glycosylation occurs. By altering this trafficking pathway, our model produces predominantly unmodified PrP^{C}, providing an ideal system to investigate whether post-translational modifications are essential for the remarkable propagation speed of bank vole-adapted CWD, the fastest known prion strain (Di Bari et al., 2013).

The GPI-less model showed complete susceptibility to CWD-vole infection, achieving 100 % attack rate despite low PrP^{C} expression levels. The extended incubation periods observed were expected, given both the low PrP^{C} expression and the mismatch between the GPI-anchored, fully glycosylated inoculum and the unmodified host PrP^{C}. To ensure complete adaptation to the GPI-less environment, we performed three serial passages, following established protocols (Aguilar-Calvo et al., 2017). The consistent 100 % attack rate across all passages, combined with a significant reduction in incubation time by the second passage, indicated successful strain adaptation. Although the third passage animals were culled before clinical onset due to concurrent health issues, preventing assessment of further incubation period shortening, the experiment achieved its primary objectives: complete strain adaptation to the GPI-less environment and elimination of the original inoculum's influence.

The neuropathological phenotype in our GPI-less model aligned with previous observations in anchorless systems (Aguilar-Calvo et al., 2017; Chesebro et al., 2005; Priola and Lawson, 2001; Rangel et al., 2014; Stöhr et al., 2011), showing a distinctive pattern of PrP^{res} accumulation. Large extracellular PrP^{res} deposits with radial arrangement appeared in perivascular, subependymal, and submeningeal spaces (Fig. 2). These deposits reached peak abundance during the second passage, when animals progressed to terminal disease stages, demonstrating successful strain adaptation. While the third passage showed similar numbers of deposits, their smaller size likely reflected the earlier euthanasia timepoint rather than altered strain properties. This pattern of abundant extracellular plaques contrasted markedly with the subtle PrP^{res} accumulation seen in conventional CWD-vole infected TgVole mice, where only sparse punctate deposits were visible in neurons and neuropil under high magnification (40×).

The identical PrP^{C} sequence in both models allows us to attribute the phenotypic differences specifically to the absence of membrane anchoring. Our findings suggest that anchorless PrP^{res} deposits exhibit reduced neurotoxicity compared to their membrane-bound counterparts. While these deposits maintain infectivity and transmissibility, they appear to cause clinical disease only after extensive accumulation overwhelms neuronal homeostasis. Several mechanisms could explain this reduced pathogenicity: First, membrane-bound PrP^{res} facilitates efficient conversion by maintaining close proximity to newly synthesized PrP^{C}. Second, membrane association enables interaction with key receptors that trigger neurotoxic cascades, such as the p75 neurotrophin receptor (Della-Bianca et al., 2001; Marco-Salazar et al., 2014). Third, membrane localization promotes cell-to-cell spread (Vilette et al., 2018), a mechanism notably absent in the anchorless model.

Additionally, two alternative mechanisms warrant consideration: GPI-less PrP^{res} may preferentially form large polymeric assemblies with reduced neurotoxicity compared to smaller oligomers (Chesebro et al., 2005; Silveira et al., 2005), or GPI-anchored PrP^{C} might serve as an essential mediator of PrP^{Sc} neurotoxicity, as suggested by PrP-knockout grafting studies (Brandner et al., 1996). Supporting this latter hypothesis, our back-passage experiments showing rapid disease progression in TgVole (1×) mice suggest that the reduced toxicity stems from the absence of membrane-bound PrP^{C} rather than intrinsic properties of the GPI-less prions themselves.

Previous studies demonstrated that mouse-adapted CWD undergoes substantial modifications when propagated in a GPI-less model (Aguilar-Calvo et al., 2017), raising the question of whether the unique characteristics of vole-adapted CWD would similarly be altered. To address this, we conducted back passages of our GPI-less adapted strain into TgVole (1×) mice, a model known to support rapid CWD-vole propagation with incubation periods under 60 days (Table 1). The initial back passage showed an incubation period of 82 ± 3 dpi, longer than typical

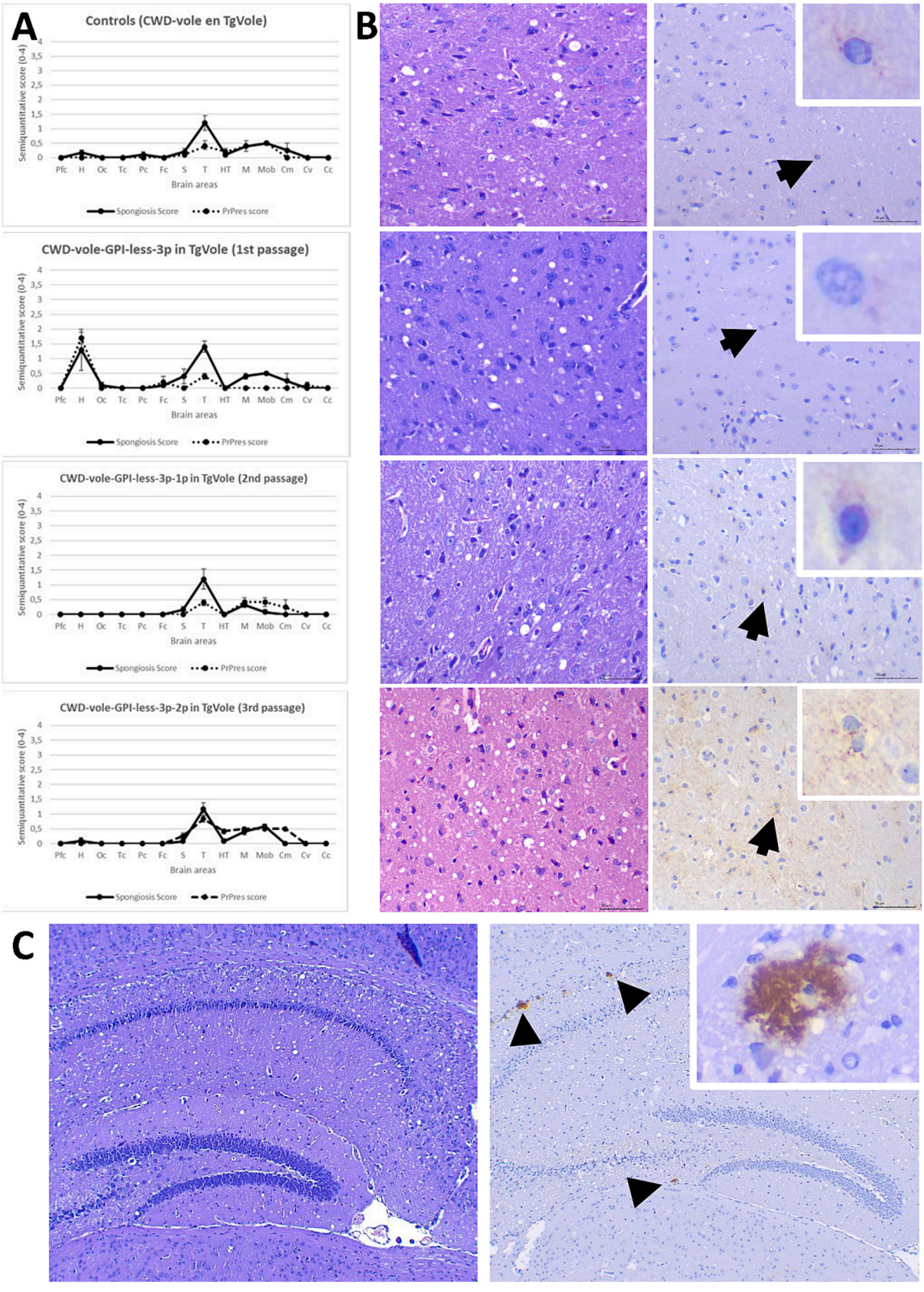

(caption on next page)

Fig. 3. Neuropathological characterization of the back-passage of GPI-less adapted CWD-vole in TgVole(1×) mice. **A)** Brain lesion and PrP^{res} deposit distribution profiles for the bank vole adapted CWD (CWD-Vole) in TgVole(1×) mice, top row and three sequential bioassays of the third passage of CWD-vole in TgVole-GPI-less mice, back passaged in TgVole(1×) mice. Brain lesion profiles and PrP^{res} deposition profiles represent the mean semi-quantitative scoring (0 -absence of lesion- to 4 -maximum intensity-, vertical axis) and error bars are the standard error of the mean of the spongiform lesions (continuous black line) and the immunohistochemical labelling of PrP^{res} deposits (dashed line) against 14 brain regions (Pfc: piriform cortex, H: hippocampus, Oc: occipital cortex, Tc: temporal cortex, Pc: parietal cortex, Fc: frontal cortex, S: striatum, T: thalamus, HT: hypothalamus, M: mesencephalon, Mob: medulla oblongata, Cm: cerebellar nuclei, Cv: cerebellar vermis, Cc: cerebellar cortex). **B)** Haematoxylin-eosin (H&E) staining of the thalamus of representative mice evidencing mild to moderate spongiform lesion on the left column and, on the right column, PrP^{res} immunostaining with the monoclonal antibody 6C2 (1:1000) where discreet small punctiform PrP^{res} deposits stained in brown (arrows and digitally enlarged in the inserts). **C)** Detail of the lesions (H&E stain, left) and plaque-like immunostained PrP^{res} deposits (6C2, 1:1000) observed in the hippocampus of a few animals of the first back passage (arrowheads, and digitally enlarged in the insert). (For interpretation of the references to colour in this figure legend, the reader is referred to the web version of this article.)

CWD-vole infections. However, subsequent passages demonstrated progressive shortening of incubation times of 64 ± 3 dpi and 67 ± 3 dpi. These final incubation periods matched those of the original CWD-vole strain (Kruskal-Wallis test, p-value = 0.06), indicating that the core biological strain properties remained intact despite prolonged propagation in a GPI-less environment.

Neuropathological and biochemical analyses of TgVole (1×) mice revealed striking similarities between animals inoculated with original CWD-vole and those receiving the GPI-less adapted strain (second and third back-passages). However, the initial back-passage showed distinctive features in three out of five animals: hippocampal spongiform lesions accompanied by small plaque-like deposits in the alveus layer (Fig. 3C). These unique characteristics might be explained by the concurrent propagation of an atypical strain, likely emerging during prolonged incubation periods in the TgVole-GPI-less model. This observation aligns with previous reports of spontaneous atypical prion formation in models expressing the bank vole 109I polymorphism. Such spontaneous strains typically emerge late in life (200–600 days), with timing dependent on PrP^{C} expression levels (Otero et al., 2019; Stöhr et al., 2011; Vidal et al., 2022; Watts et al., 2016, 2012). Notably, when directly inoculated into TgVole (4×) mice, these atypical strains show incubation periods around 120 dpi (Otero et al., 2019). Our results suggest a competitive propagation scenario during the initial back passage, where both the classical CWD-vole strain and an atypical component coexisted. The highly susceptible TgVole model apparently supported propagation of both strains initially. However, in subsequent passages, a selective pressure resulted in the emergence of a pure classical CWD-vole phenotype, as evidenced by the consistent neuropathological and biochemical profiles observed in all animals from second and third passages.

5. Conclusions

Our findings demonstrate that the remarkable propagation properties of CWD-vole, the fastest known prion strain, persist in the absence of glycosylation and GPI anchoring, suggesting that these effects are primarily determined by the protein's misfolded structure, independent of post-translational modifications. Although some strain-specific phenotypic features may be modulated by post-translational modifications, as evidenced by the slower propagation speed in GPI-less models, the core biological effects remain determined by the protein's misfolded structure. These results have important implications for prion research methodology. They validate the use of our PMSA-based system for generating recombinant prions *in vitro* (Eraña et al., 2024, 2023), which produces unmodified proteins with diverse biological effects (*i.e.* strain-specific properties) out of one given recombinant *PRNP* sequence. This approach enables large-scale production of pure misfolded prion proteins, essential for detailed structural studies. A crucial next step is the propagation of this GPI-less, predominantly unglycosylated strain using recombinant protein, which would enable structural studies and deeper understanding of the molecular basis underlying its extraordinary properties. Combined with recent advances in cryo-EM technology, these tools will allow to further unravel the structural basis of prion strain diversity (Manka et al., 2023a,b).

Supplementary data to this article can be found online at https://doi.org/10.1016/j.nbd.2025.106894.

Glossary

BSE	bovine spongiform encephalopathy
BV	bank vole
CJD	Creutzfeldt Jackob disease
Cryo-EM	Cryo-electron microscopy
CWD	chronic wasting disease
GPI	glicosyl phosphatidyl inositol
GSS	Gerstmann-Sträussler-Scheinker syndrome
PrP^{C}	cellular prion protein
PrP^{res}	resistant prion protein
PRNP	gene encoding for PrP^{C}
sCJD	sporadic CJD
PBS	phosphate buffered saline
PI-PLC	phosphatidylinositol-specific phospholipase C
PIRIBS	parallel in-register intermolecular β-sheet
PK	proteinase K
PMCA	protein misfolding cyclic amplification
PMSA	protein misfolding shaking amplification
TSE	transmissible spongiform encephalopathies
w/v	weight/volume

Credit authorship contribution statement

Enric Vidal: Supervision, Methodology, Investigation, Funding acquisition, Formal analysis, Data curation, Conceptualization. **Hasier Eraña:** Validation, Supervision, Methodology, Investigation, Formal analysis, Data curation, Conceptualization. **Jorge M. Charco:** Methodology, Investigation, Formal analysis, Data curation. **Nuria L. Lorenzo:** Methodology, Investigation, Formal analysis. **Samanta Giler:** Methodology, Investigation. **Montserrat Ordóñez:** Supervision, Methodology, Investigation, Formal analysis. **Eva Fernández-Muñoz:** Methodology, Investigation. **Maitena San-Juan-Ansoleaga:** Methodology, Investigation. **Glenn C. Telling:** Validation, Supervision, Methodology, Investigation, Formal analysis, Conceptualization. **Manuel A. Sánchez-Martín:** Methodology, Investigation. **Mariví Geijo:** Methodology, Investigation. **Jesús R. Requena:** Validation, Supervision, Investigation, Formal analysis, Conceptualization. **Joaquín Castilla:** Validation, Supervision, Methodology, Investigation, Funding acquisition, Formal analysis, Conceptualization.

Ethics approval and consent to participate

TgVole (1×) (FVB/N.129Ola-Tg (Prnp-Bvole109I)C594PRC/Cicb) and TgVole-GPI-less (B6&CBA.129Ola-Tg(Prnp-Vo109I-GPILess)1Sala/Cicb) founder mice were generated at Transgenic Facility of the University of Salamanca (Spain) and breeding colonies were kept on a 12:12 light/dark cycle, receiving food and water *ad libitum* at CIC bioGUNE (Spain). Animals were inoculated at the Center for Experimental Biomedicine (CEBEGA - University of Santiago de Compostela) and Neiker - Basque Institute for Agricultural Research and Development

(code NEIKER-OEBA-2021-003 from the centre's Ethics Committee and with authorisation DFB/BFA-2021/49 from the competent authority). All experiments involving animals in Spain adhered to the guidelines included in the Spanish law "Real Decreto 53/2013 de 1 de febrero" on protection of animals used for experimentation and other scientific purposes, which is based on the European Directive 2010/63/UE on Laboratory Animal Protection. The project was approved by the Ethical Committees on Animal Welfare (project codes assigned by the Ethical Committee CIC bioGUNE- P-CBG-CBBA-0519 (breeding) and P-CBG-CBBA-0612 (inoculations), and CEBEGA- 15005/16/006) and performed under their supervision.

Declaration of Generative AI and AI-assisted technologies in the writing process

During the preparation of this work the author(s) did not use AI or AI-assisted technologies.

Funding sources

The present work was partially funded by three different grants awarded by "Agencia Estatal de Investigación, Ministerio de Ciencia e Innovación" (Spanish Government), grant numbers PID2021-122201OB-C21 and PID2021-1222010B-C22, and co-financed by the European Regional Development Fund (ERDF). EFA031/01 NEURO-COOP, which is co-funded at 65 % by the European Union through Programa Interreg VI-A España-Francia-Andorra (POCTEFA 2021–2027). Additional funding was provided by the Instituto de Salud Carlos III (ISCIII), grant number AC21_2/00024 as member of a JPND grant JPND-2021-650-130. Additionally, CICbioGUNE currently holds a Severo Ochoa Excellence accreditation, CEX2021-001136-S, also funded by MCIN/AEI/10.13039/501100011033. Transgenic Facility, directed by M.A. S-M, is supported by Instituto de Salud Carlos III (ISCIII), co-funded by the European Union grant PT23/00123. The funders had no role in study design, data collection and analysis, decision to publish, or preparation of the manuscript.

Declaration of competing interest

Authors have read the journal's policy and have the following competing interests to declare: Authors Hasier Eraña and Jorge M. Charco are employed by the commercial company ATLAS Molecular Pharma SL. This does not alter our adherence to all Journal policies on sharing data and materials and did not influence in any way the work reported in this manuscript. The rest of the authors declare no competing interests.

Acknowledgments

The authors would like to thank the following for their support: the IKERBasque Foundation; the Vivarium and Maintenance personnel from CIC bioGUNE, for their outstanding assistance; María de la Sierra Espinar and the rest of the IRTA-CReSA BSL3 facility personnel for their excellent technical support; and the staff of the biocontainment units at Neiker and CEBEGA for their excellent care and maintenance of the animals. The authors wish to thank Umberto Agrimi and Romolo Nonno for providing bank vole I109 brain samples and the CWD-vole isolate propagated in *Myodes glareolus*.

Data availability

Data will be made available on request.

References

Aguilar-Calvo, P., Xiao, X., Bett, C., Eraña, H., Soldau, K., Castilla, J., Nilsson, K.P.R., Surewicz, W.K., Sigurdson, C.J., 2017. Post-translational modifications in PrP expand the conformational diversity of prions in vivo. Sci. Rep. 7. https://doi.org/10.1038/srep43295.

Bett, C., Kurt, T.D., Lucero, M., Trejo, M., Rozemuller, A.J., Kong, Q., Nilsson, K.P.R., Masliah, E., Oldstone, M.B., Sigurdson, C.J., 2013. Defining the conformational features of anchorless, poorly neuroinvasive prions. PLoS Pathog. 9. https://doi.org/10.1371/journal.ppat.1003280.

Borchelt, D.R., Davis, J., Fischer, M., Lee, M.K., Slunt, H.H., Ratovitsky, T., Regard, J., Copeland, N.G., Jenkins, N.A., Sisodia, S.S., Price, D.L., 1996. A vector for expressing foreign genes in the brains and hearts of transgenic mice. Genet. Anal. 13, 159–163. https://doi.org/10.1016/S1050-3862(96)00167-2.

Brandner, S., Raeber, A., Sailer, A., Blättler, T., Fischer, M., Weissmann, C., Aguzzi, A., 1996. Normal host prion protein (PrPC) is required for scrapie spread within the central nervous system. Proc. Natl. Acad. Sci. USA 93, 13148–13151. https://doi.org/10.1073/PNAS.93.23.13148.

Cancellotti, E., Bradford, B.M., Tuzi, N.L., Hickey, R.D., Brown, D., Brown, K.L., Barron, R.M., Kisielewski, D., Piccardo, P., Manson, J.C., 2010. Glycosylation of PrP C determines timing of neuroinvasion and targeting in the brain following transmissible spongiform encephalopathy infection by a peripheral route. J. Virol. 84. https://doi.org/10.1128/jvi.02374-09.

Castilla, J., Gutiérrez Adán, A., Brun, A., Pintado, B., Ramírez, M.A., Parra, B., Doyle, D., Rogers, M., Salguero, F.J., Sánchez, C., Sánchez-Vizcaíno, J.M., Torres, J.M., 2003. Early detection of PrPres in BSE-infected bovine PrP transgenic mice. Arch. Virol. 148, 677–691. https://doi.org/10.1007/s00705-002-0958-4.

Castilla, J., Gutierrez-Adan, A., Brun, A., Pintado, B., Salguero, F.J., Parra, B., Segundo, F.D., Ramirez, M.A., Rabano, A., Cano, M.J., Torres, J.M., 2005. Transgenic mice expressing bovine PrP with a four extra repeat octapeptide insert mutation show a spontaneous, non-transmissible, neurodegenerative disease and an expedited course of BSE infection. FEBS Lett. 579, 6237–6246.

Chesebro, B., Trifilo, M., Race, R., Meade-White, K., Teng, C., LaCasse, R., Raymond, L., Favara, C., Baron, G., Priola, S., Caughey, B., Masliah, E., Oldstone, M., 2005. Anchorless prion protein results in infectious amyloid disease without clinical scrapie. Science 308, 1435–1439. https://doi.org/10.1126/SCIENCE.1110837.

Collinge, J., Clarke, A.R., 2007. A general model of prion strains and their pathogenicity. Science 318, 930–936. https://doi.org/10.1126/science.1138718.

Della-Bianca, V., Rossi, F., Armato, U., Dal-Pra, I., Costantini, C., Perini, G., Politi, V., Della Valle, G., 2001. Neurotrophin p75 receptor is involved in neuronal damage by prion peptide-(106-126). J. Biol. Chem. 276, 38929–38933. https://doi.org/10.1074/jbc.M107454200.

Di Bari, M.A., Nonno, R., Castilla, J., D'Agostino, C., Pirisinu, L., Riccardi, G., Conte, M., Richt, J., Kunkle, R., Langeveld, J., Vaccari, G., Agrimi, U., 2013. Chronic wasting disease in bank voles: characterisation of the shortest incubation time model for prion diseases. PLoS Pathog. 9. https://doi.org/10.1371/JOURNAL.PPAT.1003219.

Eraña, H., Charco, J.M., Di Bari, M.A., Díaz-Domínguez, C.M., López-Moreno, R., Vidal, E., González-Miranda, E., Pérez-Castro, M.A., García-Martínez, S., Bravo, S., Fernández-Borges, N., Geijo, M., D'Agostino, C., Garrido, J., Bian, J., König, A., Uluca-Yazgi, B., Sabate, R., Khaychuk, V., Vanni, I., Telling, G.C., Heise, H., Nonno, R., Requena, J.R., Castilla, J., 2019. Development of a new largely scalable in vitro prion propagation method for the production of infectious recombinant prions for high resolution structural studies. PLoS Pathog. 15, e1008117. https://doi.org/10.1371/JOURNAL.PPAT.1008117.

Eraña, H., Díaz-Domínguez, C.M., Charco, J.M., Vidal, E., González-Miranda, E., Pérez-Castro, M.A., Piñeiro, P., López-Moreno, R., Sampedro-Torres-Quevedo, C., Fernández-Veiga, L., Tasis-Galarza, J., Lorenzo, N.L., Santini-Santiago, A., Lázaro, M., García-Martínez, S., Gonçalves-Anjo, N., San-Juan-Ansoleaga, M., Galarza-Ahumada, J., Fernández-Muñoz, E., Giler, S., Valle, M., Telling, G.C., Geijó, M., Requena, J.R., Castilla, J., 2023. Understanding the key features of the spontaneous formation of bona fide prions through a novel methodology that enables their swift and consistent generation. Acta Neuropathol. Commun. 11. https://doi.org/10.1186/S40478-023-01640-8.

Eraña, H., Sampedro-Torres-Quevedo, C., Charco, J.M., Díaz-Domínguez, C.M., Peccati, F., San-Juan-Ansoleaga, M., Vidal, E., Gonçalves-Anjo, N., Pérez-Castro, M. A., González-Miranda, E., Piñeiro, P., Fernández-Veiga, L., Galarza-Ahumada, J., Fernández-Muñoz, E., Perez de Nanclares, G., Telling, G., Geijo, M., Jiménez-Osés, G., Castilla, J., 2024. A protein misfolding shaking amplification-based method for the spontaneous generation of hundreds of bona fide prions. Nat. Commun. 15. https://doi.org/10.1038/S41467-024-46360-2.

Hoyt, F., Alam, P., Artikis, E., Schwartz, C.L., Hughson, A.G., Race, B., Baune, C., Raymond, G.J., Baron, G.S., Kraus, A., Caughey, B., 2022. Cryo-EM of prion strains from the same genotype of host identifies conformational determinants. PLoS Pathog. 18. https://doi.org/10.1371/JOURNAL.PPAT.1010947.

Jansen, C., Parchi, P., Capellari, S., Vermeij, A.J., Corrado, P., Baas, F., Strammiello, R., Van Gool, W.A., Van Swieten, J.C., Rozemuller, A.J.M., 2010. Prion protein amyloidosis with divergent phenotype associated with two novel nonsense mutations in PRNP. Acta Neuropathol. 119, 189–197. https://doi.org/10.1007/S00401-009-0609-X.

Kim, J. Il, Surewicz, K., Gambetti, P., Surewicz, W.K., 2009. The role of glycophosphatidylinositol anchor in the amplification of the scrapie isoform of prion protein in vitro. FEBS Lett. 583. https://doi.org/10.1016/j.febslet.2009.10.049.

Kraus, A., Hoyt, F., Schwartz, C.L., Hansen, B., Artikis, E., Hughson, A.G., Raymond, G.J., Race, B., Baron, G.S., Caughey, B., 2021. High-resolution structure and strain comparison of infectious mammalian prions. Mol. Cell 81, 4540–4551.e6. https://doi.org/10.1016/j.molcel.2021.08.011.

Lawson, V.A., Collins, S.J., Masters, C.L., Hill, A.F., 2005. Prion protein glycosylation. J. Neurochem. 93, 793–801. https://doi.org/10.1111/j.1471-4159.2005.03104.x.
Makarava, N., Baskakov, I.V., 2023. Role of sialylation of N-linked glycans in prion pathogenesis. Cell Tissue Res. https://doi.org/10.1007/s00441-022-03584-2.
Manka, Szymon W., Wenborn, A., Betts, J., Joiner, S., Saibil, H.R., Collinge, J., Wadsworth, J.D.F., 2023a. A structural basis for prion strain diversity. Nat. Chem. Biol. 19, 607–613. https://doi.org/10.1038/s41589-022-01229-7.
Manka, Szymon W., Wenborn, A., Collinge, J., Wadsworth, J.D.F., 2023b. Prion strains viewed through the lens of cryo-EM. Cell Tissue Res. 392, 167–178. https://doi.org/10.1007/S00441-022-03676-Z.
Manson, J.C., Clarke, A.R., Hooper, M.L., Aitchison, L., McConnell, I., Hope, J., 1994. 129/Ola mice carrying a null mutation in PrP that abolishes mRNA production are developmentally normal. Mol. Neurobiol. 8, 121–127. https://doi.org/10.1007/BF02780662.
Marco-Salazar, P., Márquez, M., Fondevila, D., Rabanal, R.M., Torres, J.M., Pumarola, M., Vidal, E., 2014. Mapping of neurotrophins and their receptors in the adult mouse brain and their role in the pathogenesis of a transgenic murine model of bovine spongiform encephalopathy. J. Comp. Pathol. 150. https://doi.org/10.1016/j.jcpa.2013.11.209.
Otero, A., Hedman, C., Fernández-Borges, N., Eraña, H., Marín, B., Monzón, M., Sánchez-Martín, M.A., Nonno, R., Badiola, J.J., Bolea, R., Castilla, J., 2019. A single amino acid substitution, found in mammals with low susceptibility to prion diseases, delays propagation of two prion strains in highly susceptible transgenic mouse models. Mol. Neurobiol. 56, 6501–6511. https://doi.org/10.1007/S12035-019-1535-0/FIGURES/4.
Otero, A., Betancor, M., Eraña, H., Borges, N.F., Lucas, J.J., Badiola, J.J., Castilla, J., Bolea, R., 2021. Prion-associated neurodegeneration causes both endoplasmic reticulum stress and proteasome impairment in a murine model of spontaneous disease. Int. J. Mol. Sci. 22, 1–21. https://doi.org/10.3390/ijms22010465.
Otero, A., Barrio, T., Eraña, H., Charco, J.M., Betancor, M., Díaz-Domínguez, C.M., Marín, B., Andréoletti, O., Torres, J.M., Kong, Q., Badiola, J.J., Bolea, R., Castilla, J., 2022. Glycans are not necessary to maintain the pathobiological features of bovine spongiform encephalopathy. PLoS Pathog. 18. https://doi.org/10.1371/journal.ppat.1010900.
Parchi, P., Gambetti, P., 1995. Human prion diseases. Curr. Opin. Neurol. 8, 286–293.
Piro, J.R., Harris, B.T., Nishina, K., Soto, C., Morales, R., Rees, J.R., Supattapone, S., 2009. Prion protein glycosylation is not required for strain-specific neurotropism. J. Virol. 83, 5321–5328. https://doi.org/10.1128/JVI.02502-08.
Priola, S.A., Lawson, V.A., 2001. Glycosylation influences cross-species formation of protease-resistant prion protein. EMBO J. 20, 6692–6699. https://doi.org/10.1093/EMBOJ/20.23.6692.
Prusiner, S.B., 1991. Molecular biology of prion diseases. Science (1979) 252, 1515–1522.
Rangel, A., Race, B., Phillips, K., Striebel, J., Kurtz, N., Chesebro, B., 2014. Distinct patterns of spread of prion infection in brains of mice expressing anchorless or anchored forms of prion protein. Acta Neuropathol. Commun. 2. https://doi.org/10.1186/2051-5960-2-8.
Rudd, P.M., Merry, A.H., Wormald, M.R., Dwek, R.A., 2002. Glycosylation and prion protein. Curr. Opin. Struct. Biol. 12, 578–586. https://doi.org/10.1016/S0959-440X(02)00377-9.
Shen, P., Dang, J., Wang, Z., Zhang, W., Yuan, J., Lang, Y., Ding, M., Mitchell, M., Kong, Q., Feng, J., Rozemuller, A.J.M., Cui, L., Petersen, R.B., Zou, W.Q., 2021. Characterization of anchorless human PrP with Q227X stop mutation linked to Gerstmann-Sträussler-Scheinker syndrome in vivo and in vitro. Mol. Neurobiol. 58, 21–33. https://doi.org/10.1007/S12035-020-02098-8.
Silveira, J.R., Raymond, G.J., Hughson, A.G., Race, R.E., Sim, V.L., Hayes, S.F., Caughey, B., 2005. The most infectious prion protein particles. Nature 437, 257–261.
Stöhr, J., Watts, J.C., Legname, G., Oehler, A., Lemus, A., Nguyen, H.O.B., Sussman, J., Wille, H., DeArmond, S.J., Prusiner, S.B., Giles, K., 2011. Spontaneous generation of anchorless prions in transgenic mice. Proc. Natl. Acad. Sci. USA 108, 21223–21228. https://doi.org/10.1073/PNAS.1117827108.
Tuzi, N.L., Cancellotti, E., Baybutt, H., Blackford, L., Bradford, B., Plinston, C., Coghill, A., Hart, P., Piccardo, P., Barron, R.M., Manson, J.C., 2008. Host PrP glycosylation: a major factor determining the outcome of prion infection. PLoS Biol. 6. https://doi.org/10.1371/journal.pbio.0060100.
Vidal, E., Sánchez-Martín, M.A., Eraña, H., Lázaro, S.P., Pérez-Castro, M.A., Otero, A., Charco, J.M., Marín, B., López-Moreno, R., Díaz-Domínguez, C.M., Geijo, M., Ordóñez, M., Cantero, G., di Bari, M., Lorenzo, N.L., Pirisinu, L., d'Agostino, C., Torres, J.M., Béringue, V., Telling, G., Badiola, J.J., Pumarola, M., Bolea, R., Nonno, R., Requena, J.R., Castilla, J., 2022. Bona fide atypical scrapie faithfully reproduced for the first time in a rodent model. Acta Neuropathol. Commun. 10. https://doi.org/10.1186/S40478-022-01477-7.
Vilette, D., Courte, J., Peyrin, J.M., Coudert, L., Schaeffer, L., Andréoletti, O., Leblanc, P., 2018. Cellular mechanisms responsible for cell-to-cell spreading of prions. Cell. Mol. Life Sci. 75, 2557–2574. https://doi.org/10.1007/S00018-018-2823-Y.
Watts, J.C., Giles, K., Stöhr, J., Oehler, A., Bhardwaj, S., Grillo, S.K., Patel, S., DeArmond, S.J., Prusiner, S.B., 2012. Spontaneous generation of rapidly transmissible prions in transgenic mice expressing wild-type bank vole prion protein. Proc. Natl. Acad. Sci. USA 109, 3498–3503. https://doi.org/10.1073/PNAS.1121556109.
Watts, J.C., Giles, K., Bourkas, M.E.C., Patel, S., Oehler, A., Gavidia, M., Bhardwaj, S., Lee, J., Prusiner, S.B., 2016. Towards authentic transgenic mouse models of heritable PrP prion diseases. Acta Neuropathol. 132, 593–610. https://doi.org/10.1007/S00401-016-1585-6.
Wells, G.A., Scott, A.C., Johnson, C.T., Gunning, R.F., Hancock, R.D., Jeffrey, M., Dawson, M., Bradley, R., 1987. A novel progressive spongiform encephalopathy in cattle. Vet. Rec. 121, 419–420.
Wenborn, A., Terry, C., Gros, N., Joiner, S., D'Castro, L., Panico, S., Sells, J., Cronier, S., Linehan, J.M., Brandner, S., Saibil, H.R., Collinge, J., Wadsworth, J.D.F., 2015. A novel and rapid method for obtaining high titre intact prion strains from mammalian brain. Sci Rep 5. https://doi.org/10.1038/SREP10062.
Williams, E.S., 2005. Chronic wasting disease. Vet. Pathol. 42, 530–549.
Wiseman, F.K., Cancellotti, E., Piccardo, P., Iremonger, K., Boyle, A., Brown, D., Ironside, J.W., Manson, J.C., Diack, A.B., 2015. The glycosylation status of PrP C is a key factor in determining transmissible spongiform encephalopathy transmission between species. J. Virol. 89. https://doi.org/10.1128/jvi.02296-14.
Yuan, J., Zhan, Y.A., Abskharon, R., Xiao, X., Martinez, M.C., Zhou, X., Kneale, G., Mikol, J., Lehmann, S., Surewicz, W.K., Castilla, J., Steyaert, J., Zhang, S., Kong, Q., Petersen, R.B., Wohlkonig, A., Zou, W.Q., 2013. Recombinant human prion protein inhibits prion propagation in vitro. Sci. Rep. 3. https://doi.org/10.1038/srep02911.